

Magneto hydrodynamic approach of non-Newtonian blood flow with magnetic particles in stenosed artery*

I. A. MIRZA¹, M. ABDULHAMEED^{2,†}, S. SHAFIE³

1. Abdus Salam School of Mathematical Sciences,
Government College University, Lahore 54000, Pakistan;
2. School of Science and Technology, Federal Polytechnic, P. M. B., Bauchi 0231, Nigeria;
3. Department of Mathematical Sciences, Faculty of Science,
Universiti Teknologi, Skudai 81310, Malaysia

Abstract The non-Newtonian blood flow, together with magnetic particles in a stenosed artery, is studied using a magneto-hydrodynamic approach. The wall slip condition is also considered. Approximate solutions are obtained in series forms under the assumption that the Womersley frequency parameter has small values. Using an integral transform method, analytical solutions for any values of the Womersley parameter are obtained. Numerical simulations are performed using MATHCAD to study the influence of stenosis and magnetic field on the flow parameters. When entering the stenosed area, blood velocity increases slightly, but increases considerably and reaches its maximum value in the stenosis throat. It is concluded that the magnitude of axial velocity varies considerably when the applied magnetic field is strong. The magnitude of maximum fluid velocity is high in the case of weak magnetic fields. This is due to the Lorentz's force that opposes motion of an electrically conducting fluid. The effect of externally transverse magnetic field is to decelerate the flow of blood. The shear stress consistently decreases in the presence of a magnetic field with increasing intensity.

Key words Bingham plastic fluid, magnetic particle, blood flow, magneto hydrodynamics, artery stenosis

Chinese Library Classification R318

2010 Mathematics Subject Classification 76Zxx, 76Wxx, 35Cxx

Nomenclature

A_0 ,	amplitude of pressure gradient steady (N/s^3);	A_1 ,	amplitude of pressure gradient oscillations (N/s^3);
B ,	magnetic flux intensity (T);	$\bar{R}(\bar{z})$,	radius of artery in stenosed region (m);
B_0 ,	applied magnetic field;	$\bar{R}(0)$,	radius of normal artery (m);
b_0 ,	amplitude of body acceleration (N/s^3);	E ,	electric field intensity (V/m);
\bar{L}_0 ,	length of stenosis (m);	E_{hdp} ,	effective hydrodynamic radius;

* Received Aug. 14, 2016 / Revised Oct. 8, 2016

Project supported by the Tertiary Education Trust Fund of Nigeria (TETFund) (No. FPTB-2016)

† Corresponding author, E-mail: moallahyidi@gmail.com

F_{em} ,	electromagnetic force (N/m ³);	F_b ,	buoyancy force (N/m ³);
F_m ,	magnetic force (N/m ³);	F_{blood} ,	fluidic force (N/m ³);
G ,	$\frac{M\mu}{\rho R_0^2 K}$ particle mass parameter;	N ,	number of magnetic particles per unit volume;
$\bar{\psi}$,	$(\frac{\xi_s}{R(0)L_0^m}) \frac{m^{m/(m-1)}}{(m-1)}$ maximum height of stenosis;	p ,	pressure gradient (Pa);
Ha ,	$\sqrt{\frac{\sigma}{\mu}} B_0 \bar{R}_0$ Hartmann number;	R_1 ,	$\frac{KN\bar{R}_0^2}{\mu}$ particle concentration parameter;
J ,	current density (A/m ²);	\bar{d} ,	stenosis location;
\mathbf{k} ,	unit vector of z -direction;	r ,	radius (m);
K ,	Stokes constant;	t ,	time (s);
\bar{L} ,	length of stenosis (m);	u ,	velocity of blood (m/s);
m ,	stenosis shape parameter ($m \geq 2$);	\mathbf{v} ,	velocity field;
M ,	mass of single nanoparticles (Kg);	v ,	velocity of magnetic particles (m/s);
		$\bar{G}(\bar{t})$,	body acceleration.

Greek letters

α^2 ,	$\frac{\bar{w}_p \bar{R}_0^2 \rho}{\mu}$ Womersley frequency parameter;	σ ,	electrical conductivity (S/m);
μ_0 ,	magnetic permeability (H/m);	$\bar{\omega}_b$,	$2\pi \bar{f}_b$ frequency (Hz);
$\bar{\tau}$,	shear stress;	\bar{f}_b ,	pulse rate frequency (Hz);
$\bar{\tau}_y$,	yield stress;	φ ,	lead angle of body acceleration;
ρ ,	density of blood (kg/m ³);	$\bar{\omega}_p$,	$2\pi \bar{f}_p$ heart pressure frequency;
μ ,	dynamic viscosity of blood (kg/(ms));	\bar{f}_p ,	pulse rate frequency (Hz).

1 Introduction

Arterial stenosis is a serious medical problem as an obstruction in the blood artery that disturbs the normal blood circulation^[1-2]. Several authors have studied the blood flow through artery with stenosis using Newtonian or non-Newtonian fluid models^[3-6]. Nagarani and Sarojamma^[7] have analyzed the pulsatile flow of the blood through a stenosed artery under the effect of body acceleration using the Casson fluid model. They found that the yield stress of fluid and the body acceleration strongly influence the flow rate in a stenosed artery. The effects of stenosis length on resistance to flow of the blood considered as a Bingham fluid, through an artery with multiple stenoses have been studied by Yadav and Kumar^[8]. They obtained that the flow resistance decreases if the shape parameter increases and the flow resistance increases if increasing the height/length of stenosis. Srikanth and Tedesse^[9] have studied the pulsatile blood flow in a multiple stenotic artery using the micropolar fluid model and the couple-stress fluid model. Siddiqui et al.^[10] have considered the blood flow through a stenosed artery with body acceleration and oscillating pressure gradient, using the Bingham plastic fluid model. They obtained analytic solution to the blood velocity, flow rate, shear stress, and effective blood viscosity. The study reveals that the blood velocity and the flow rate increase with the body acceleration, while the effective blood viscosity and shear stress decrease. Applications to the targeting of a magnetic drug are an important subject of research in medical treatment methods for the effective targeting and delivery of drugs to a specific target area^[11-13]. Furlani and Ng^[14] have studied a mathematical model for transport of the therapeutic magnetic nanoparticles in the human microvasculature. Furlani and Furlani^[15], Sharma et al.^[16] have studied the motion of magnetic nanoparticles in blood vessels under the influence of magnetic field. Based on the magneto-hydrodynamic approach, Sharma et al.^[17] analyzed the flow of blood along with magnetic particles in a cylindrical tube under effects of the magnetic field and pressure waveform. Nehad et al.^[18] extended the work of Sharma^[17] to a model with time-fractional derivatives of Caputo type. Other interesting topics were studied in Refs. [19]–[25].

In the present paper, we consider a blood model along with magnetic particles, starting from

the model studied by Siddiqui et al.^[10], in which the blood is considered as a non-Newtonian Bingham plastic fluid. In their paper, Siddiqui and his collaborators have studied the effects of the body acceleration, oscillating pressure gradient along the flow direction and of the slip velocity on the fluid velocity and on the volumetric flow rate. They have not considered the influence of the external magnetic field. Also, they determined only the approximate solution under the assumption of small values of the Womersley parameter, α .

The aim of this paper is to study the blood flow along with magnetic particles through an arterial stenosis under the influence of a magnetic field perpendicular to the flow direction, an oscillating pressure waveform in the axial direction and the body acceleration. We assume that the blood is flowing in the axial direction and the magnetic particles are uniformly distributed throughout the blood. Using suitable non-dimensional variables, we have formulated the dimensionless initial-boundary value problem which governs the flow. Approximate solutions for the axial fluid velocity, particles velocity, and shear stress are obtained for small values of the Womersley parameter. In order to eliminate this restrictive condition, we have determined an analytical solution using the Laplace and finite Hankel transforms. These analytical solutions are new in the literature and can be used to study the fluid flow parameters for any value of the Womersley parameter.

The influence of magnetic field on the blood velocity and the shear stress was numerically analyzed using the MATHCAD software. We found that the flow parameters through the stenotic arteries are significantly disturbed compared to flow through the arteries without stenosis. In the non-stenosed area the blood flows with constant velocity. The blood velocity slightly increases at the inlet of the stenosed area, then increases considerably and reaches its maximum value in the stenosis throat. It is obtained that, the axial velocity has a considerable variation in magnitude when the applied magnetic field is stronger. For the variation of the magnetic field intensity, the magnitude of maximum value of the fluid velocity becomes higher in the case of weak magnetic fields. This behavior is due to the Lorentz's force which opposes the motion of an electrically conducting fluid. The effect of externally magnetic field is to decelerate the flow of blood. The shear stress consistently decreases in the presence of a magnetic field with increasing intensity. The study of the shear stress distribution plays an important role, because, the deterioration of the arterial wall is related to the generation of tension on the arterial walls.

2 Mathematical model formulation

We consider the pulsatile blood flow along with magnetic particles through a stenosed artery with slip velocity at the constricted wall. The blood is considered as a non-Newtonian fluid of Bingham plastic model ^[10,17,26–28], in the presence of an applied magnetic field, an oscillating pressure gradient in the axial direction, and periodic body acceleration. The magnetic particles are flowing along the axis of the artery and are uniformly distributed throughout in the blood.

2.1 Model equations

We suppose that the stenosis of the arterial wall (see Fig.1) is a function of the axial coordinate z , given by the following equation (see Siddiqui et al.^[10]):

$$\frac{\bar{R}(\bar{z})}{\bar{R}(0)} = \begin{cases} 1 - \bar{\psi}(\bar{L}_0^{m-1}(\bar{z} - \bar{d}) - (\bar{z} - \bar{d})^m), & \bar{d} \leq \bar{z} \leq \bar{d} + \bar{L}_0, \\ 1, & \text{otherwise,} \end{cases} \quad (1)$$

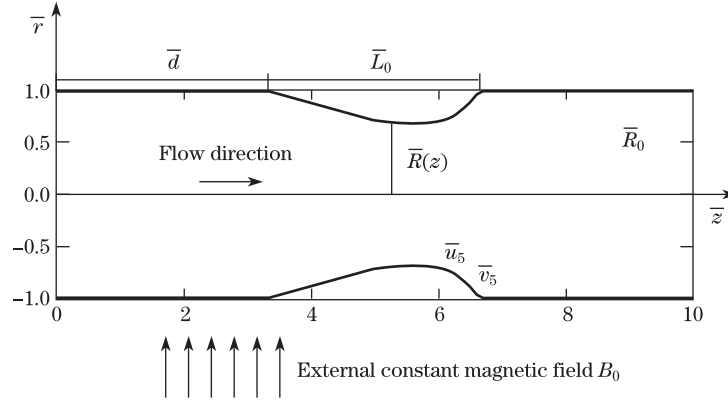


Fig. 1 Geometry of stenosis

where $\bar{R}(\bar{z})$ is the radius of the artery in the stenosed region, $\bar{R}(0) = \bar{R}_0$ is the radius of the normal artery, \bar{L}_0 is the length of the stenosis, \bar{d} is the stenosis location, and $\bar{\psi} = \left(\frac{\xi_s}{\bar{R}(0)\bar{L}_0^m}\right) \frac{m^{m/(m-1)}}{(m-1)}$ is the maximum height of the stenosis at $\bar{z} = \bar{d} + (\bar{L}_0/m^{m/(m-1)})$ such that $\xi_s/\bar{R}(0) < 1$.

The model for the blood motion consists of Navier-Stokes equations, the constitutive equations of the Bingham plastic fluid, and the Maxwell equations of the magnetic field is as follows:

$$\nabla \cdot \mathbf{B} = 0, \quad \nabla \times \mathbf{B} = \mu_0 \mathbf{J}, \quad \nabla \times \mathbf{E} = -\frac{\partial \mathbf{B}}{\partial t}, \tag{2}$$

where \mathbf{B} is the magnetic flux intensity, μ_0 is the magnetic permeability, \mathbf{E} is the electric field intensity, and \mathbf{J} is the current density given by

$$\mathbf{J} = \sigma(\mathbf{E} + \mathbf{v} \times \mathbf{B}), \tag{3}$$

σ is the electrical conductivity, and \mathbf{v} is the velocity field.

The electromagnetic body force \mathbf{F}_{em} is defined as

$$\mathbf{F}_{em} = \mathbf{J} \times \mathbf{B} = \sigma(\mathbf{E} + \mathbf{v} \times \mathbf{B}) \times \mathbf{B} = \sigma B_0^2 \bar{u}(r, t) \mathbf{k}, \tag{4}$$

where \mathbf{k} is the unite vector of the z -direction, and $\mathbf{v} = \bar{u}(r, t) \mathbf{k}$ is the axial velocity of the blood. The electromagnetic body force \mathbf{F}_{em} is inserted in the momentum equation (5).

Under the assumption that the ratio of the maximum height of the stenosis and the radius of the non-stenotic region, respectively, the ratio of the radius of non-stenotic region and the length of stenosis are much smaller than unity, the governing equation of motion and stress tensor are given by Ref. [23]:

Momentum equation

$$\rho \left(\frac{\partial \bar{u}}{\partial \bar{t}} \right) = - \left(\frac{\partial \bar{p}}{\partial \bar{z}} \right) - \left(\frac{1}{\bar{r}} \right) \frac{\partial}{\partial \bar{r}} (\bar{r} \bar{\tau}) + \bar{G}(\bar{t}) + KN(\bar{v} - \bar{u}) - \sigma B_0^2 \bar{u}. \tag{5}$$

The constitutive Bingham plastic model stress tensor $\bar{\tau}$ of the forms^[10]

$$\bar{\tau} = \bar{\tau}_y - \mu \left(\frac{\partial \bar{u}}{\partial \bar{r}} \right) \quad \text{for} \quad \bar{\tau} \geq \bar{\tau}_y, \tag{6}$$

$$\frac{\partial \bar{u}}{\partial \bar{r}} = 0 \quad \text{for} \quad \bar{\tau} < \bar{\tau}_y, \tag{7}$$

where \bar{u} is the axial velocity of blood, \bar{v} is the velocity of particles, \bar{t} is the time, \bar{p} is the pressure, $\bar{\tau}$ is the shear stress, $\bar{G}(\bar{t})$ is the body acceleration, B_0 is the externally applied

constant magnetic field, $\bar{\tau}_y$ is the yield stress, ρ is the density of blood, μ is the dynamic viscosity of the blood, K is the Stokes constant, N is the number of magnetic particles per unit volume, and $\frac{KN}{\rho}(\bar{v} - \bar{u})$ is the interaction between motion of blood and magnetic particles. We considered the Reynolds number of the relative velocity is small; therefore the force between blood and magnetic particles is proportional to the relative velocity.

The periodic body acceleration $\bar{G}(\bar{t})$ and pressure gradient $\frac{\partial \bar{p}}{\partial \bar{z}}(\bar{z}, \bar{t})$ for $t > 0$, which appears in (5), have the expression of the following forms^[10]:

$$\bar{G}(\bar{t}) = b_0 \cos(\bar{\omega}_b \bar{t} + \varphi), \quad (8)$$

$$-\frac{\partial \bar{p}}{\partial \bar{z}}(\bar{z}, \bar{t}) = A_0 + A_1 \cos(\bar{\omega}_p \bar{t}), \quad (9)$$

where $\bar{\omega}_b = 2\pi\bar{f}_b$ is the frequency, \bar{f}_b is the pulse rate frequency, φ is the lead angle of the body acceleration with respect to the pressure gradient, $\bar{\omega}_p = 2\pi\bar{f}_p$ is the heart pressure frequency, \bar{f}_p is the pulse rate frequency, A_0 is the amplitude of the steady state pressure gradient, and A_1 is the amplitude of the oscillating pressure gradient.

The motion of nanoparticles in the vascular system is governed by a number of forces^[16]. In the current investigation, we consider the fluidic force and the unsteady flow analysis are implemented. Therefore, the motion of magnetic single particle is governed by Newton's law for dynamic of particle motion

$$M \frac{\partial \bar{v}}{\partial t} = \sum F_{\text{ext}}, \quad (10)$$

where M is the mass of the single nanoparticles and $\sum F_{\text{ext}} = F_m + F_b + F_{\text{blood}}$ represents all the external forces exerted on the particle from which F_m is the magnetic force, F_b is the buoyancy force, and F_{blood} is the fluidic force.

The fluidic force experienced by a particle, assuming a Reynolds number $\Re \leq 1$, is predicted using Stokes's law for viscous drag on a sphere

$$F_{\text{blood}} = -6\pi\mu E_{\text{hyd,p}}(\bar{v} - \bar{u}), \quad (11)$$

where $E_{\text{hyd,p}}$ is the effective hydrodynamic radius of the particle, \bar{v} is the particle velocity, the $-$ sign indicates that the fluidic force acts opposite to the direction of the particles motion. We predict particle motion when only the force on the particle is fluidic and no buoyancy force

$$M \frac{\partial \bar{v}}{\partial t} = K(\bar{u} - \bar{v}), \quad (12)$$

where $K = 6\pi\mu E_{\text{hyd,p}}$ is the Stokes constant.

2.2 Initial and boundary conditions

For the proposed problem, we consider the following initial and boundary condition:

$$\bar{u} = \bar{v} = 0, \quad \text{at } \bar{t} = 0, \quad (13)$$

$$\bar{u} = \bar{u}_s \quad \text{and} \quad \bar{v} = \bar{v}_s, \quad \text{at } \bar{r} = \bar{R}(\bar{z}), \quad (14)$$

$$\bar{\tau} \text{ is finite, at } \bar{r} = 0, \quad (15)$$

where \bar{u}_s, \bar{v}_s are the slip velocities at the stenotic walls (see Fig. 1).

The dimensionless forms of the governing equations are obtained by considering the following

dimensionless variables:

$$\left\{ \begin{array}{l} u = \frac{\bar{u}}{A_0 \bar{R}_0^2 / (4\mu)}, \quad v = \frac{\bar{v}}{A_0 \bar{R}_0^2 / (4\mu)}, \quad \theta = \frac{\bar{\tau}_y}{A_0 \bar{R}_0 / 2}, \quad R(z) = \frac{\bar{R}(z)}{\bar{R}_0}, \\ t = \bar{t} \bar{w}_p, \quad A = \frac{A_1}{A_0}, \quad \xi_s = \frac{\bar{\xi}_s}{\bar{R}_0}, \quad B = \frac{b_0}{A_0}, \quad r = \frac{\bar{r}}{\bar{R}_0}, \\ u_s = \frac{\bar{u}_s}{A_0 \bar{R}_0^2 / (4\mu)}, \quad v_s = \frac{\bar{v}_s}{A_0 \bar{R}_0^2 / (4\mu)}, \quad \omega = \frac{\bar{\omega}_b}{\bar{w}_p}, \quad \tau = \frac{\bar{\tau}}{A_0 \bar{R}_0 / 2}. \end{array} \right. \tag{16}$$

(5), (12), (6), and (7) become

$$\alpha^2 \frac{\partial u}{\partial t} = f(t) + R_1(v - u) - \frac{2}{r} \frac{\partial}{\partial r}(r\tau) - Ha^2 u, \tag{17}$$

$$\alpha^2 \frac{\partial v}{\partial t} = \frac{1}{G}(u - v), \tag{18}$$

$$\tau = \theta - \frac{1}{2} \frac{\partial u}{\partial r} \quad \text{for } \tau \geq \theta, \tag{19}$$

$$\frac{\partial u}{\partial r} = 0 \quad \text{for } \tau < \theta. \tag{20}$$

The dimensionless initial and boundary conditions are

$$u = v = 0, \quad \text{at } t = 0, \tag{21}$$

$$u = u_s, \quad v = v_s, \quad \text{at } r = R(z), \tag{22}$$

$$\tau \text{ is finite, at } r = 0, \tag{23}$$

where $\alpha^2 = \frac{\bar{w}_p \bar{R}_0^2 \rho}{\mu}$, α is the Womersley frequency parameter, $Ha = \sqrt{\frac{\sigma}{\mu}} B_0 \bar{R}_0$ is the Hartmann number, $R_1 = \frac{KN\bar{R}_0^2}{\mu}$ is the particle concentration parameter, $G = \frac{M\mu}{\rho \bar{R}_0^2 K}$ is the particle mass parameter, and $f(t) = 4((1 + A \cos t) + B \cos(\omega t + \varphi))$,

It is important to point out that, if the particle concentration parameter is zero ($R_1 = 0$) and no magnetic field effect ($Ha = 0$), then (17) represents the classical model which was given by Ref. [10].

3 Solution technique

Let the blood velocity u , the magnetic particles velocity v , and the shear stress τ be expressed in the forms

$$u(z, r, t) = u_0(z, r, t) + \alpha^2 u_1(z, r, t) + \dots, \tag{24}$$

$$\tau(z, r, t) = \tau_0(z, r, t) + \alpha^2 \tau_1(z, r, t) + \dots, \tag{25}$$

$$v(z, r, t) = v_0(z, r, t) + \alpha^2 v_1(z, r, t) + \dots. \tag{26}$$

Substituting u , v , and τ from (24)–(26) into (17)–(19) and equating the coefficients of α^0 and α^2 , respectively, we obtain

$$f(t) + R_1(v_0 - u_0) - Ha^2 u_0 - \frac{2}{r} \frac{\partial}{\partial r}(r\tau_0) = 0, \tag{27}$$

$$u_0 - v_0 = 0, \tag{28}$$

$$\tau_0 = \theta - \frac{1}{2} \frac{\partial u_0}{\partial r}, \tag{29}$$

and

$$\frac{\partial u_0}{\partial t} = R_1(v_1 - u_1) - Ha^2 u_1 - \frac{2}{r} \frac{\partial}{\partial r}(r\tau_1), \quad (30)$$

$$G \frac{\partial v_0}{\partial t} = u_1 - v_1, \quad (31)$$

$$\tau_1 = -\frac{1}{2} \frac{\partial u_1}{\partial r}. \quad (32)$$

Substituting (28) and (29) into (27), we obtain

$$\frac{2}{r} \frac{\partial}{\partial r} \left(r \left(\theta - \frac{1}{2} \frac{\partial u_0}{\partial r} \right) \right) + Ha^2 u_0 - f(t) = 0. \quad (33)$$

Making the change of function

$$Ha^2 u_0 - f(t) = 2F_0(r, z, t), \quad (34)$$

(33) becomes

$$r \frac{\partial^2 F_0}{\partial r^2} + \frac{\partial F_0}{\partial r} - Ha^2 r F_0 = \theta Ha^2. \quad (35)$$

We seek the solution of (35) in the form of power series as

$$F_0 = \sum_{n=0}^{\infty} C_n(z, t) r^n. \quad (36)$$

It follows that, the general terms for C_{2n+1} and C_{2n+2} can be immediately obtained, respectively as:

$$C_{2n+1} = (2Ha)^{2n} \left(\frac{n!}{(2n+1)} \right)^2 C_1 = (2Ha)^{2n} \left(\frac{n!}{(2n+1)!} \right)^2 \theta Ha^2, \quad (37)$$

$$C_{2n+2} = \left(\frac{Ha}{2} \right)^{2(n+1)} \frac{C_0}{((n+1)!)^2}, \quad n = 0, 1, 2, \dots \quad (38)$$

The function $F_0(r, z, t)$ is expressed as follows:

$$\begin{aligned} F_0(r, z, t) &= C_0 + \sum_{n=0}^{\infty} C_{2n+1} r^{2n+1} + \sum_{n=0}^{\infty} C_{2n+2} r^{2n+2} \\ &= C_0 + \theta Ha^2 \sum_{n=0}^{\infty} (2Ha)^{2n} \left(\frac{n!}{(2n+1)!} \right) r^{2n+1} \\ &\quad + C_0 \sum_{n=0}^{\infty} \left(\frac{Ha}{2} \right)^{2(n+1)} \frac{r^{2n+2}}{((n+1)!)^2}, \end{aligned} \quad (39)$$

which can be written in the simpler form

$$F_0(r, z, t) = C_0(z, t) I_0(Ha r) + \frac{\pi \theta}{2} \sum_{n=0}^{\infty} \frac{1}{(\Gamma(n + \frac{3}{2}))^2} \left(\frac{rHa}{2} \right)^{2n+1}. \quad (40)$$

The solution u_0 can be expressed as

$$u_0 = \frac{2F_0(r, z, t) + f(t)}{Ha^2}. \quad (41)$$

Using the boundary condition $u_0 = u_s$ at $r = R(z)$, we obtain

$$C_0(z, t) = \frac{1}{2} \left(\frac{Ha^2 u_s - f(t) - \pi \theta Ha^2 b(z)}{I_0(Ha R(z))} \right) \tag{42}$$

with $b(z) = \sum_{n=0}^{\infty} \frac{1}{(\Gamma(n+\frac{3}{2}))^2} (\frac{Ha R(z)}{2})^{2n+1}$ and I_0 is the modified Bessel function of order zero.

The solution of v_0 and τ_0 can be readily expressed as

$$v_0 = u_0, \tag{43}$$

$$\tau_0 = \theta - \frac{1}{Ha^2} \frac{\partial F_0(r, z, t)}{\partial r}. \tag{44}$$

Following the same procedure for obtaining $u_0, v_0,$ and $\tau_0, u_1, v_1,$ and τ_1 can be achieved similarly.

Substituting (31) and (32) into (30), we obtain

$$r \frac{\partial^2 u_1}{\partial r^2} + \frac{\partial u_1}{\partial r} - Ha^2 u_1 r = \left(1 - \sum_{n=0}^{\infty} \left(\frac{Ha}{2} \right)^{2(n+1)} \frac{r^{2n+2}}{((n+1)!)^2} \right) h(t)r, \tag{45}$$

where

$$h(t) = \frac{4(1 + RG) df(t)}{Ha^2 dt}. \tag{46}$$

The solution of the problem (45), (46) with the boundary condition $u_1(R(z), z, t) = 0$ is

$$\begin{aligned} u_1(r, z, t) = & \frac{h(t)}{4} r^2 + D_0(z, t) + D_0(z, t) \sum_{n=1}^{\infty} \left(\frac{Ha}{2} \right)^{2n+2} \frac{r^{2n+2}}{((n+1)!)^2} \\ & + \sum_{n=1}^{\infty} D_{2n+1} r^{2n+1}, \quad D_0 = - \frac{\frac{h(t)}{4} R^2(z) + \sum_{n=1}^{\infty} R^{2n+1}(z)}{1 + \sum_{n=0}^{\infty} \left(\frac{Ha}{2} \right)^{2n+2} \frac{R^{2n+2}(z)}{((n+1)!)^2}}. \end{aligned} \tag{47}$$

The solutions of v_1 and τ_1 are immediately as follows:

$$v_1 = u_1 - G \frac{\partial v_0}{\partial t}, \quad \tau_1 = -\frac{1}{2} \frac{\partial u_1}{\partial r}. \tag{48}$$

The above obtained solution represents an approximate solution, and it was determined under assumption that the Womersley number α has small values. This is a very restrictive condition. In order to have a more general solution, we have determined an analytical solution by means of the integral transform method (Laplace and finite Hankel transforms).

Applying the Laplace transform, with respect to the time variable t , to (17), (18), then applying the finite Hankel transform of order zero, with respect to the radial variable r and applying the inverse transforms we have the velocity $u(z, r, t)$ in the following form:

$$\begin{aligned} u(z, r, t) = & u_s - \frac{2u_s}{R(z)} \sum_{n=1}^{\infty} \frac{J_0(rr_n(z))}{r_n(z)J_1(R(z)r_n(z))} M_n(z, t) \\ & + \frac{2}{R^2(z)} \sum_{n=1}^{\infty} \frac{J_0(rr_n(z))}{J_1^2(R(z)r_n(z))} \int_0^t N_n(z, \tau) S_n(z, t - \tau) d\tau, \end{aligned} \tag{49}$$

where

$$M_n(z, t) = 1 - \frac{\alpha^2 G r_n^2(z) q_{1n}(z) + r_n^2(z) e^{q_{1n}(z)t} - 1}{\alpha^4 G (q_{1n}(z) - q_{2n}(z)) q_{1n}(z)} + \frac{\alpha^2 G r_n^2(z) q_{2n}(z) + r_n^2(z) e^{q_{2n}(z)t} - 1}{\alpha^4 G (q_{1n}(z) - q_{2n}(z)) q_{2n}(z)}, \quad (50)$$

$$N_n(z, t) = \frac{\alpha^2 G q_{1n}(z) + 1}{\alpha^4 G (q_{1n}(z) - q_{2n}(z))} e^{q_{1n}(z)t} - \frac{\alpha^2 G q_{2n}(z) + 1}{\alpha^4 G (q_{1n}(z) - q_{2n}(z))} e^{q_{2n}(z)t}, \quad (51)$$

$$S_n(z, t) = 4\rho_n(z)(1 + A \cos(t) + B \cos(\omega t + \phi)) + \sigma_n(z), \quad (52)$$

$$\rho_n(z) = \frac{R(z)}{r_n(z)} J_1(R(z)r_n(z)), \quad \sigma_n(z) = -2\theta \int_0^{R(z)} J_0(rr_n(z)) dr, \quad (53)$$

$$q_{1n}(z), q_{2n}(z) = \frac{-(1 + G(R + Ha^2 + r_n^2(z)))}{2\alpha^2 G} \pm \frac{\sqrt{(1 + G(R + Ha^2 + r_n^2(z)))^2 - 4G(Ha^2 + r_n^2(z))}}{2\alpha^2 G}, \quad (54)$$

and $r_n(z)$ are the positive roots of the transcendental equation $J_0(R(z)r_n) = 0$.

4 Results and discussion

In this paper, we have investigated the mathematical model that represents non-Newtonian flow of the blood through a stenosed artery, in the presence of an external magnetic field perpendicular to the flow direction. Periodic body acceleration and an oscillating pressure gradient along the flow direction are considered by the function $f(t)$, periodic in time (see Fig. 2). Under assumption of small values of the Womersley number, the approximate solutions to the axial velocity of fluid and suspended particles as well as to the shear stress were determined. In order to obtain information regarding the flow parameters, we carried out numerical calculations using the software MATHCAD. The computed results are exhibited through Figs. 3–5, in order to have their quantitative estimates. The profiles of axial fluid velocity and of the shear stress were plotted versus axial z -coordinate, for different values of the radial coordinate r (few coaxial fluid layers) and for different values of the time t or, of the Hartmann number Ha . For numerical simulations we used the following values for the system parameters^[8,10]:

$$\alpha = 0.2, \quad R_1 = 0.8, \quad G = 2, \quad \frac{\bar{d}}{R_0} = \frac{10}{3}, \quad \frac{\bar{L}_0}{R_0} = \frac{10}{3}, \quad A = 0.5, \quad B = 0.065, \quad \frac{\xi_s}{R_0} = \frac{1}{3},$$

$$\omega = 5, \quad \varphi = 1.571, \quad n = 6, \quad u_s = 1.5, \quad \theta = 0.75.$$

Function $f(t)$ has the expression

$$f(t) = 4(0.05 + A \cos(t) + B \cos(\omega t + \varphi)).$$

The diagram of the pulsating function $f(t)$ is sketched in Fig. 2. In the numerical calculation, we used for the time t values $t=1$ and $t=4$. The first value corresponds to the descending branch of the diagram, respectively; the second value corresponds to the ascending branch of the diagram plotted in Fig. 2.

Figures 3 and 4 show the variation of dimensionless axial velocity with the axial coordinate z , for different values of the Hartman number and time t . As we expected, in the absence of stenosis, the axial blood velocity is constant at each instant t and in each circular fluid layer. In the stenosed area of the circular tube, the fluid velocity has a strong variation, namely, the axial fluid velocity increases. The stenosis height affects the flow velocity. The fluid velocity increases slightly in the stenotic area but, increases considerable and reaches its maximum

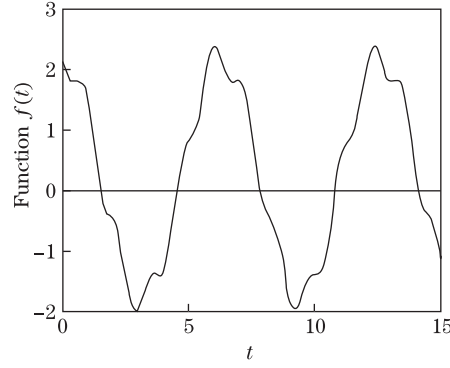


Fig. 2 Function $f(t)$ -oscillating pressure gradient and body acceleration

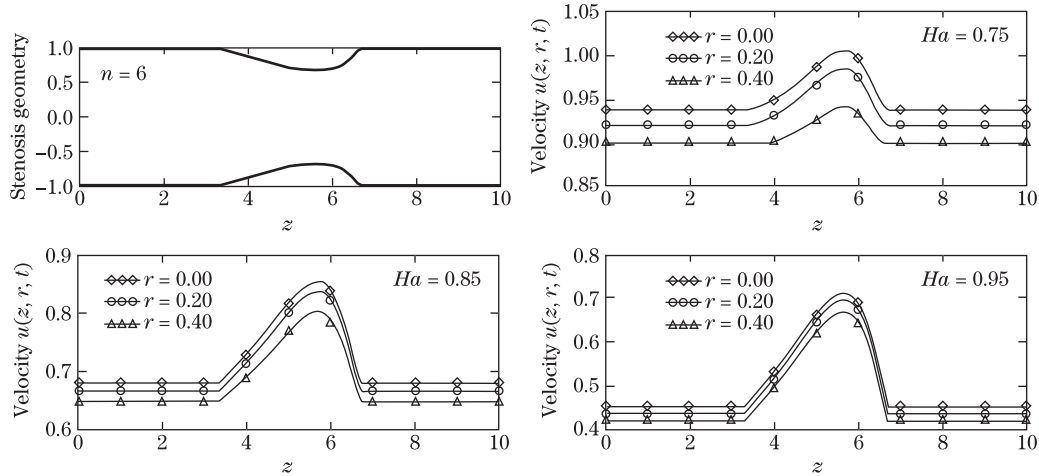


Fig. 3 Profiles of axial velocity $u(z, r, t)$ for time $t=1$ and for different values of Hartman number Ha

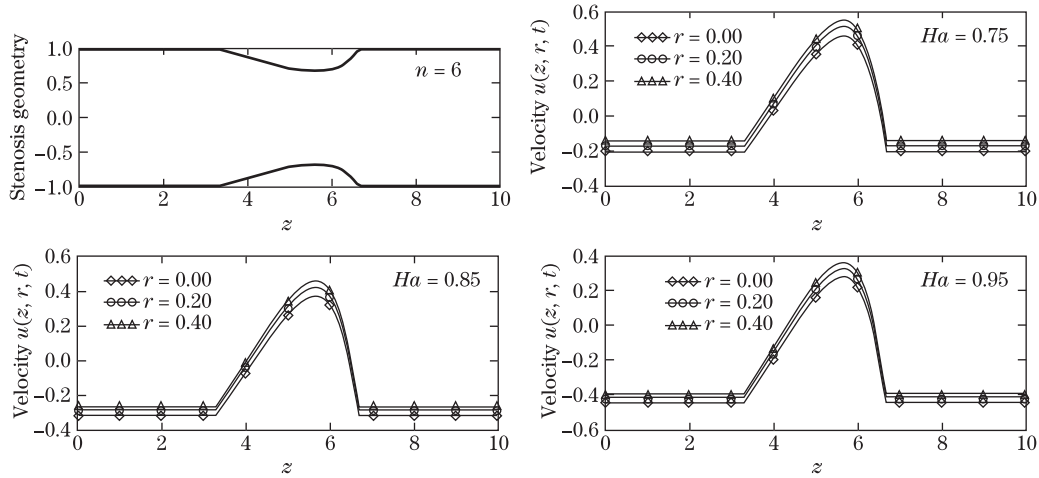


Fig. 4 Profiles of axial velocity $u(z, r, t)$ for time $t=4$ and for different values of Hartman number Ha

there where the stenosis height is maximum, i.e., in the area where the orifice of flowing has the smallest diameter. One may, also, observe from these figures that when the Hartman number increases (the applied magnetic field is stronger), the axial velocity has a considerable variation

in magnitude. For the variation of the magnetic field intensity, the magnitude of the maximum value of the fluid velocity becomes higher in the case of lower values of the Hartman number. Therefore, in the case of weak magnetic fields. This behavior is due to the Lorentz's force which opposes the motion of an electrically conducting fluid. The effect of externally applied transverse magnetic field is to decelerate the flow of blood.

Figure 5 exhibits how the shear stress is perturbed at the different Hartman numbers Ha , different radial positions and also, at different axial positions of the stenosed artery. It is observed from Fig. 5 that, the shear stress consistently decreases in the presence of a magnetic

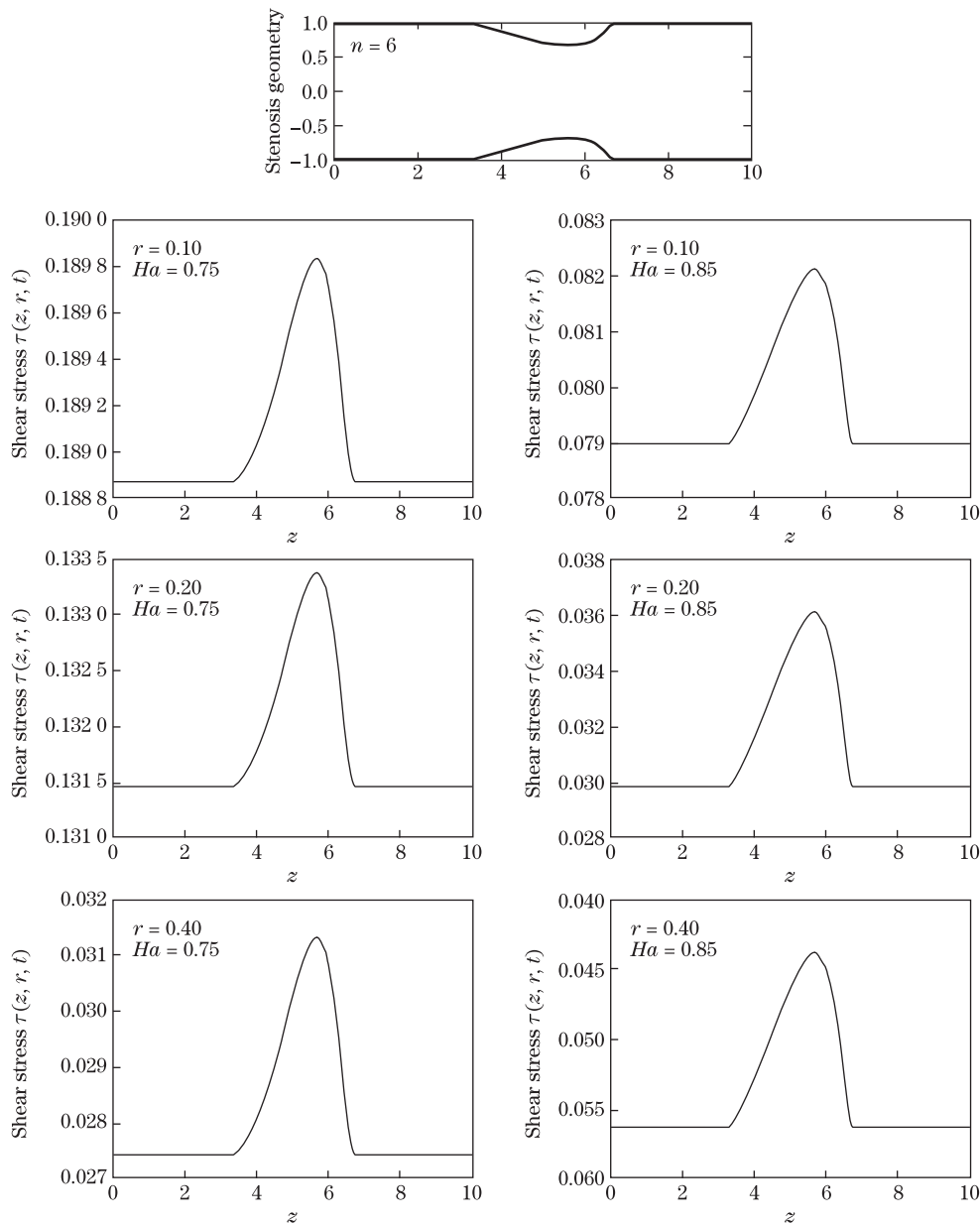


Fig. 5 Profiles of shear stress $\tau(z, r, t)$ for time $t=1$, $\theta=0.75$ and for different values of Hartman number Ha

field with increasing intensity. The peak stress occurs at the throat of the stenosis. The shear stress distribution plays an important role, because, the deterioration of the arterial wall is related to the generation of tension on the arterial walls.

Obviously, (24) is an approximate solution to fluid velocity and it can be used only for small values of the Womersley number α . The solution given by (49) is true for all values of the parameter α , and therefore it is more suitable for proposed problem. However, from Table 1 it is observed that an acceptable agreement was found between numerical results to both solutions.

Table 1 Comparison between solutions $u(z, r, t)$ given by (24) and (49) for $\alpha=0.45$, $r=0.3$, $t=0.5$, $Ha=0.75$, $R=0.8$, $G=2$, $\omega=0.86$, $\varphi=0.628$, $A=0.05$, $B=0.065$, and $\theta=0.75$

z	$u(z, r, t); (24)$	$u(z, r, t); (49)$
3.0	0.539	0.534
3.4	0.529	0.525
3.8	0.447	0.436
4.2	0.376	0.366
4.6	0.315	0.302
5.0	0.301	0.287
5.4	0.237	0.245
5.8	0.233	0.218
6.2	0.280	0.302
6.6	0.476	0.456

5 Conclusions

In this research, we formulated a mathematical model describing pulsating blood flow along with magnetic particles through stenosed artery with applied magnetic field, oscillating pressure gradient, external body acceleration, and slip velocity. The governing coupled flow equations for both blood and magnetic particles are solved analytically and simulated on MATHCAD software. The main results of the current study are summarized as follows:

- (i) The blood velocity and magnetic particles velocity can be controlled by adjusting the magnetic parameter.
- (ii) The blood flow is constant with respect to the axial coordinate z , in the absence of stenosis.
- (iii) In the stenosed area of the artery the blood velocity has a strong variation.
- (iv) The shear stress has variation from a constant in the area without stenosis and much higher in the layers located close to the longitudinal axis of the artery
- (v) The peak velocity and peak shear stress occur at the throat of the stenosis.

Acknowledgements Authors are grateful to reviewers for their observations and suggestions that led to the paper improvement. The first author is grateful to Abdus Salam School of Mathematical Sciences, Lahore for support in the scientific research.

References

- [1] Hogan, H. A. and Henriksen, M. An evaluation of a micropolar model for blood flow through an idealized stenosis. *Journal of Biomechanics*, **22**, 211–218 (1989)
- [2] Bali, R. and Awasthi, U. Effect of a magnetic field on the resistance to blood flow through stenotic artery. *Applied Mathematics and Computation*, **188**, 1635–1641 (2007)
- [3] Sankar, D. S. and Lee, U. Mathematical modeling of pulsatile flow of non-Newtonian fluid in stenosed arteries. *Communications in Nonlinear Science and Numerical Simulation*, **14**, 2971–2981 (2009)

-
- [4] Mustapha, N., Amin, N., Chakravarty, S., and Mandal, P. K. Unsteady magnetohydrodynamic blood flow through irregular multi-stenosed arteries. *Computers in Biology and Medicine*, **39**, 896–906 (2009)
- [5] Pralhad, R. N. and Schultz, D. H. Modeling of arterial stenosis and its applications to blood diseases. *Mathematical Biosciences*, **190**, 203–220 (2004)
- [6] Sahu, M. K., Sharma, S. K., and Agrawal, A. K. Study of arterial blood flow in stenosed vessel using non-Newtonian couple stress fluid model. *International Journal of Dynamics of Fluids*, **6** (2), 248–257 (2010)
- [7] Nagarani, P. and Sarojamma, G. Effect of body acceleration on pulsatile flow of Casson fluid through a mild stenosed artery. *Korea-Australia Rheology Journal*, **48**, 189–196 (2008)
- [8] Yadav, S. S. and Kumar, K. Bingham plastic characteristic of blood flow through a generalized atherosclerotic artery with multiple stenosis. *Advance in Applied Science Research*, **3**, 3551–3557 (2012)
- [9] Srikanth, D. and Tedesse, K. Mathematical analysis of non-Newtonian fluid flow through multiple stenotic artery in the presence of catheter—a pulsatile flow. *International Journal of Nonlinear Science*, **13**, 15–27 (2012)
- [10] Siddiqui, S. U., Shah, S. R., and Geeta. A biomechanical approach to study the effect of body acceleration and slip velocity through stenotic artery. *Applied Mathematics and Computation*, **261**, 148–155 (2015)
- [11] Voltairas, P. A., Fotiadis, D. I., and Michalis, L. K. Hydrodynamics of magnetic drug targeting. *Journal of Biomechanics*, **35**, 813–821 (2002)
- [12] Ganguly, R., Gaiind, A. P., Sen, S., and Puri, I. K. Analyzing ferrofluid transport for magnetic drug targeting. *Journal of Magnetism and Magnetic Materials*, **289**, 331–334 (2005)
- [13] Banerjee, M. K., Datta, A., and Ganguly, R. Magnetic drug targeting in partly occluded blood vessels using magnetic microspheres. *Journal of Nanotechnology in Engineering and Medicine*, **1**, 1–9 (2010)
- [14] Furlani, E. P. and Ng, K.C. Analytical model of magnetic nanoparticle transport and capture in the microvasculature. *Physics Review E*, **73**, 061919 (2006)
- [15] Furlani, E. J. and Furlani, E. P. A model for predicting magnetic targeting of multifunctional particles in the microvasculature. *Journal of Magnetism and Magnetic Materials*, **312**, 187–193 (2007)
- [16] Sharma, S., Katiyar, V. K., and Singh, U. Mathematical modelling for trajectories of magnetic nanoparticles in a blood vessel under magnetic field. *Journal of Magnetism and Magnetic Materials*, **379**, 102–107 (2015)
- [17] Sharma, S., Singh, U., and Katiyar, V. K. Magnetic field effect on flow parameters of blood along with magnetic particles in a cylindrical tube. *Journal of Magnetism and Magnetic Materials*, **377**, 395–401 (2015)
- [18] Nehad, A. S., Dumitru, V., and Constantin, F. Effects of the fractional order and magnetic field on the blood flow in cylindrical domains. *Journal of Magnetism and Magnetic Materials*, **409**, 10–19 (2016)
- [19] Gayathri, K. and Shailendhra, K. Pulsatile blood flow in large arteries: comparative study of Burton’s and McDonald’s models. *Applied Mathematics and Mechanics (English Edition)*, **35**, 574–590 (2014) DOI 10.1007/s10483-014-1814-7
- [20] Hatami, M., Ghasemi, S. E., Sahebi, S. A. R., Mosayebidorcheh, S., Ganji, D. D., and Hatami, J. Investigation of third-grade non-Newtonian blood flow in arteries under periodic body acceleration using multi-step differential transformation method. *Applied Mathematics and Mechanics (English Edition)*, **36**, 1449–1458 (2015) DOI 10.1007/s10483-015-1995-7
- [21] Bennett, L. Red cell slip at a wall in vitro. *Science*, **24**, 1554–1556 (1967)
- [22] Ponalagusamy, R. Blood flow through an artery with mild stenosis: a twolayered model, different shapes of stenoses and slip velocity at the wall. *Journal of Applied Sciences*, **7**, 1071–1077 (2007)
- [23] Zaman, A., Ali, N., and Sajid, M. Slip effects on unsteady non-Newtonian blood flow through an inclined catheterized overlapping stenotic artery. *AIP Advances*, **6**, 015118 (2016)

- [24] Reddy, J. R., Srikanth, D., and Murthy, S. K. Mathematical modelling of pulsatile flow of blood through catheterized unsymmetric stenosed artery—effects of tapering angle and slip velocity. *European Journal of Mechanics B/Fluids*, **48**, 236–244 (2014)
- [25] Nadeem, S. and Ijaz, S. Theoretical examination of nanoparticles as a drug carrier with slip effects on the wall of stenosed arteries. *International Journal of Heat and Mass Transfer*, **93**, 1137–1149 (2016)
- [26] Johnson, M., and Ethier, C. R. *Problems for Biomedical Fluid Mechanics and Transport Phenomena*, Cambridge University Press, Cambridge (2013)
- [27] Ahmed, S. Bingham plastic fluid model for steady flow of blood with velocity slip tube wall in presence of magnetic field. *Asian Journal of Technology & Management Research*, **5**(1), 57–70 (2015)
- [28] Sharma, S., Kumar, R., and Gaur, A. A model for magnetic nanoparticles transport in a channel for targeted drug delivery. *Procedia Materials Science*, **10**, 44–49 (2015)